Noise Attention Learning: Enhancing Noise Robustness by Gradient Scaling

Yangdi Lu
Department of Computing and Software
McMaster University
luy100@mcmaster.ca

Yang Bo
Department of Computing and Software
McMaster University
boy2@mcmaster.ca

Wenbo He
Department of Computing and Software
McMaster University
hew11@mcmaster.ca

Abstract

Machine learning has been highly successful in data-driven applications but is often hampered when the data contains noise, especially label noise. When trained on noisy labels, deep neural networks tend to fit all noisy labels, resulting in poor generalization. To handle this problem, a common idea is to force the model to fit only clean samples rather than mislabeled ones. In this paper, we propose a simple yet effective method that automatically distinguishes the mislabeled samples and prevents the model from memorizing them, named Noise Attention Learning. In our method, we introduce an attention branch to produce attention weights based on representations of samples. This attention branch is learned to divide the samples according to the predictive power in their representations. We design the corresponding loss function that incorporates the attention weights for training the model without affecting the original learning direction. Empirical results show that most of the mislabeled samples yield significantly lower weights than the clean ones. Furthermore, our theoretical analysis shows that the gradients of training samples are dynamically scaled by the attention weights, implicitly preventing memorization of the mislabeled samples. Experimental results on two benchmarks (CIFAR-10 and CIFAR-100) with simulated label noise and three real-world noisy datasets (ANIMAL-10N, Clothing1M and Webvision) demonstrate that our approach outperforms state-of-the-art methods.

1 Introduction

With the emergence of highly-curated datasets such as ImageNet [1] and CIFAR [2], deep neural networks (DNNs) have achieved remarkable performance on many classification tasks. However, in real-world applications, it is extremely time-consuming and expensive, sometimes even impossible to label a new large-scale dataset containing fully correct annotations. To alleviate this problem, one may obtain the data with lower quality annotations efficiently through online keywords queries [3] or crowdsourcing [4], but *noisy labels* (e.g. a cat image is mislabeled as dog) are inevitably introduced consequently. Previous study [5] has empirically demonstrated that noisy labels in training data are problematic for deep neural networks, resulting in overfitting and performance degradation. Therefore, designing robust algorithms against noisy labels is of great practical importance.

Given the training data consists of clean (correctly labeled) samples and mislabeled samples, DNNs have been observed to correctly predict the true labels for all training samples during a *early learning*

36th Conference on Neural Information Processing Systems (NeurIPS 2022).

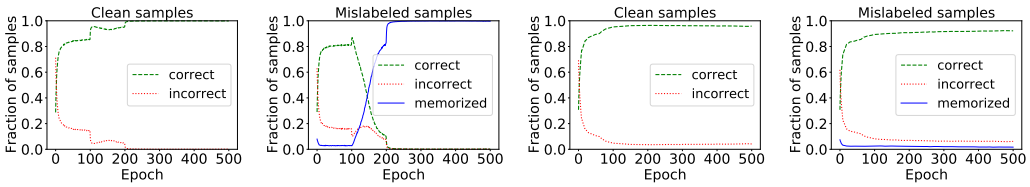

(a) CE (b) CE (c) NAL (ours) (d) NAL (ours)

Figure 1: The results of training a ResNet34 [14] with cross entropy (CE) loss and our proposed method on the CIFAR-10 with 40% symmetric noise. Plots (a) and (c) show the fraction of clean samples that are predicted correctly (green) and incorrectly (red). In contrast, plots (b) and (d) show the fraction of mislabeled samples that are predicted correctly (green), memorized (i.e. the prediction equals the wrong label, shown in blue), and incorrectly predicted as neither the true nor the labeled class (red). For clean samples, both models predict them correctly with the increasing of epochs. However, for mislabeled samples in plot (b), the model trained with CE loss first predicts the true labels correctly, but eventually memorizes all mislabeled samples. In contrast, our approach prevents memorization of mislabeled samples, allowing the model to continue learning the clean samples to attain high accuracy on all samples.

stage, and then start to make incorrect predictions as it gradually *memorizes* the mislabeled samples [6, 7] (see Figure 1(a) and 1(b)). Based on this empirical finding, many existing approaches [8–11] use the training loss or prediction confidence to identify mislabeled samples in the early learning stage, i.e., the samples with small loss or high confidence are more likely to be clean samples. After dividing the samples into clean and mislabeled sets, one can simply train the model only based on clean set [8, 11], or correct these mislabeled samples by pseudo-labels [9, 12], or treat them as unlabeled samples and train the model using semi-supervised learning algorithms [10]. However, these methods typically involve sophisticated training procedure modifications and sometimes require high computational costs.

In this paper, we propose Noise Attention Learning (NAL) which enjoys simplicity and universality from a new perspective. The core idea behind NAL is to let the model automatically differentiate the mislabeled samples from clean samples, and prevent the memorization of mislabeled samples in training. Since the memorization of DNNs has a preference for easy (clean) samples, the predictive power of a sample's representation aligns with its label cleanliness [6]. To transform this qualitative observation into a quantitive measure, we introduce an attention branch that outputs scalar attention weights to indicate the predictive power of representations. We incorporate the attention weights in our loss function, so that the attention branch can be learned to divide samples, i.e., clean samples are learned to be associated with large weights, while mislabeled ones with small weights. In this way, the proposed method does not require extra steps (e.g. modeling loss distribution [9, 10], selecting small-loss samples [8]) to separate the training set, effectively simplifying the training procedure. Theoretically, we demonstrate that NAL neutralizes the effect of the mislabeled samples on the gradient and ensures the contribution of clean samples to the whole gradient remains dominant, thereby preventing the deep neural networks from overfitting mislabeled samples.

The proposed method has a similar effect on gradients as an existing regularization method ELR [7]. In general, the performance of pure regularization methods cannot be compared to complex methods. Despite that the regularization methods can effectively hinder the memorization of mislabeled samples, the limited number of clean samples makes the model not rich enough to generalize effectively to the held-out data. To solve this problem, ELR uses temporal ensembling [13] to estimate the targets in its loss function to correctly guide the model for improving performance. Similarly, instead of directly using noisy labels as target distribution in our loss function, we adopt SELC [12] to estimate the targets, allowing the generation of more clean labels for learning sufficiency.

Empirically, we show that the proposed approach achieves better robustness than the state-of-the-art methods on two benchmarks (CIFAR-10 and CIFAR-100 [2]) with simulated label noise and three challenging datasets in noisy label literature (ANIMAL-10N [15], Clothing1M [16] and Webvision [3]) with real-world label noise. To better understand our method, we conduct many empirical analyses, including memorization analysis, gradient analysis, attention weights, quality of targets, hyperparameter sensitivity and ablation study, to verify our theoretical explanations and design goals.

2 Preliminaries

Classification with Noisy Labels. Consider the K-class classification problem in noisy-label scenario, the ground truth label y is unobservable. We only have a noisy training set $\hat{D} = \{(\boldsymbol{x}^{[i]}, \hat{y}^{[i]})\}_{i=1}^{N}$, where $\boldsymbol{x}^{[i]}$ is an input and $\hat{y}^{[i]} \in \mathcal{Y} = \{1, \ldots, K\}$ is the corresponding noisy label. We denote $\hat{\boldsymbol{y}}^{[i]} \in \{0,1\}^K$ as one-hot vector of noisy label $\hat{y}^{[i]}$. A DNN $\mathcal{N}_\theta$ maps an input $\boldsymbol{x}^{[i]}$ to a K-dimensional logits and then feeds the logits to a softmax function to obtain $\boldsymbol{p}^{[i]}$ of the conditional probability of each class. θ denotes the parameters of the DNN and $\boldsymbol{z}^{[i]} \in \mathbb{R}^{K\times 1}$ denotes the logits (i.e. pre-softmax output). We refer to it as prediction branch in this work. We have $\boldsymbol{z}^{[i]} = \mathcal{N}_\theta(\boldsymbol{x}^{[i]})$ and $\boldsymbol{p}^{[i]} = \texttt{softmax}(\boldsymbol{z}^{[i]})$. Without knowing the ground truth joint probability distribution $P(\boldsymbol{x}, y)$, the typical cross-entropy (CE) loss is often used as empirical risk to measure how well the model fits the training set $\hat{D}$ as follows:

$$\mathcal{L}_{\text{ce}} = \frac{1}{N}\sum_{i=1}^{N} \ell_{\text{ce}}(\hat{\boldsymbol{y}}^{[i]}, \boldsymbol{p}^{[i]}) = -\frac{1}{N}\sum_{i=1}^{N} (\hat{\boldsymbol{y}}^{[i]})^\top \log(\boldsymbol{p}^{[i]}). \tag{1}$$

Early Learning Phenomenon When optimizing $\mathcal{L}_{\text{ce}}$ by stochastic gradient descent (SGD), it has been observed that DNNs fit the easy (clean) samples first before memorizing of hard (mislabeled) samples [6]. Figure 1(a) and 1(b) shows this qualitative behavior. The model begins by learning to predict the true labels, even for majority of mislabeled samples, but eventually learns to predicts wrong labels due to memorization of mislabeled samples.

Label Noise Model. The generation of real-world label noise is unpredictable, a typical methodology to dealing with noisy labels is to posit a noise model and develop robust algorithms under the hypothetical noise model. The algorithms are then tested on the real-world noisy datasets to see how effective they are. A widely-accepted noise model is class-conditional noise [17, 18], where label noise is independent of input features and true labels are corrupted by a *symmetric* or *asymmetric* noise transition matrix (simulation details are in Appendix B.2). Instance-dependent noise [19, 20] is another noise model in which the noise is affected not only by the label but also by the input feature.

3 Noise Attention Learning

In this section, we present our approach NAL for learning with noisy labels. NAL consists of three key elements: (1) An attention branch based on learned representations to produce the attention weight for each training sample; (2) A noise attention loss is specifically designed to learn the attention weights; (3) A target estimation strategy to help generate more clean labels for sufficient learning.

3.1 Attention Branch based on Learned Representations

To enable the deep neural networks to produce an attention weight that reflects the quality of learned representation, we introduce an attention branch just after the penultimate layer of the original model. We denote M-dimensional penultimate layer (representation) of input $\boldsymbol{x}^{[i]}$as $H^{[i]}$. $H^{[i]}$ is shared in both prediction and attention branches. For each input, the prediction branch outputs the softmax prediction $\boldsymbol{p}^{[i]}$ as usual. The attention branch contains one fully connected layer to produce a single scalar value $h^{[i]}$, and `sigmoid` function is applied to scale it between 0 to 1. Specifically, we have $h^{[i]} = WH^{[i]} + b$, where $W \in \mathbb{R}^{1\times M}$ denotes the weights and $b \in \mathbb{R}$ denotes the bias in penultimate layer of the attention branch. We have the attention weight $\tau^{[i]}$ for each sample $\boldsymbol{x}^{[i]}$ as

$$\tau^{[i]} = \texttt{sigmoid}(h^{[i]}), \quad \tau^{[i]} \in (0,1). \tag{2}$$

Note that W and b are extra network parameters need to be learned to produce meaningful τ's. Therefore, attention weights are not fixed but dynamic during the training.

3.2 Noise Attention Loss

The early learning phenomenon reveals that the DNNs memorize the clean samples before the mislabeled samples. Therefore, clean samples are more likely to have better learned representations than mislabeled samples in the early learning phase. To enable the attention weights to automatically

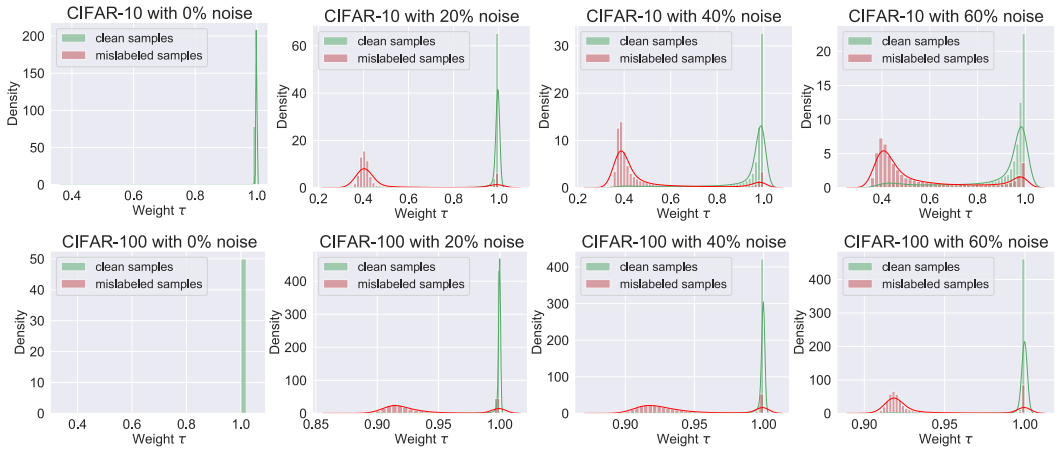

Figure 2: The distribution of attention weights on the CIFAR-10/CIFAR-100 with different ratios of symmetric label noise using ResNet34.

capture the difference of representations as well as learn the classification task, we propose a noise attention loss consisting of two terms: attention term $\mathcal{L}_{\mathrm{a}}$ and boost term $\mathcal{L}_{\mathrm{b}}$.

$$\mathcal{L}_{\mathrm{NAL}} = \mathcal{L}_{\mathrm{a}} + \lambda \mathcal{L}_{\mathrm{b}} = -\frac{1}{N}\sum_{i=1}^{N}(\hat{\boldsymbol{y}}^{[i]})^{\top}\log\big(\underbrace{\tau^{[i]}(\boldsymbol{p}^{[i]}-\hat{\boldsymbol{y}}^{[i]})+\hat{\boldsymbol{y}}^{[i]}}_{\text{perceptual shortcut}}\big) - \frac{\lambda}{N}\sum_{i=1}^{N}\log(\tau^{[i]}), \tag{3}$$

where λ is the hyperparameter. Intuitively, the attention term $\mathcal{L}_{\mathrm{a}}$ can be interpreted as a dynamic expansion of the CE loss, where the prediction is modified to 'perceptual shortcut' $\tau(\boldsymbol{p}-\hat{\boldsymbol{y}})+\hat{\boldsymbol{y}}$ (Note that many existing methods [9, 21, 22] use this linear interpolation formula to infer the label distribution, while the proposed NAL applies it to prediction distribution for learning the meaningful attention weights). Assuming no representations are corrupted and all weights $\tau \to 1$, the attention term $\mathcal{L}_{\mathrm{a}}$ reduces to exactly $\mathcal{L}_{\mathrm{ce}}$ in Eq. (1). On the contrary, when all $\tau \to 0$, the attention term $\mathcal{L}_{\mathrm{a}}$ becomes "lazy" as it produces many zero gradients.

The mechanism of attention term can be explained as follows: (1) For mislabeled samples, the model does not memorize them in the early learning phase. Therefore, their representations are under learned compared to clean samples and $(\boldsymbol{p}-\hat{\boldsymbol{y}})$ remains large. By minimizing $\mathcal{L}_{\mathrm{a}}$, it forces τ of mislabeled samples toward 0, which is treated as 'shortcut'. (2) For clean samples, the model memorizes them first, resulting in $(\boldsymbol{p}-\hat{\boldsymbol{y}}) \to \mathbf{0}$. It makes τ have no influence on minimizing $\mathcal{L}_{\mathrm{a}}$ as the prediction distribution is already equal to $\hat{\boldsymbol{y}}$. As a result, by solely minimizing $\mathcal{L}_{\mathrm{a}}$, we may obtain a trivial optimization result that the model always produces $\tau \to 0$ for any inputs. To avoid this 'lazy' learning circumstance, we have another boost term $\mathcal{L}_{\mathrm{b}}$. It can be interpreted as a binary CE loss, where the target of τ is always 1 for all inputs. By adding the boost term, the attention weights of clean samples are pushed to 1.0, and weights of mislabeled samples are still close to 0 as expected.

To verify the effectiveness of $\mathcal{L}_{\mathrm{NAL}}$ in discriminating the mislabeled samples from clean samples, we empirically analyze the weight distribution of clean and mislabeled samples with simulated symmetric noise. Figure 2 shows results on CIFAR-10 and CIFAR-100 with different ratios of symmetric noise. In 0% noise cases, we observe that all samples have weights close to 1.0, which indicates that $\mathcal{L}_{\mathrm{NAL}}$ reduced to exactly $\mathcal{L}_{\mathrm{ce}}$. Thus, the proposed loss would not affect the performance when training with clean data. At other ratios of label noise, there is a clear separation between attention weights of clean and mislabeled samples. The weights of clean samples form a spike close to 1.0, whereas the weights of most mislabeled samples are plainly less than 1.0, which satisfies our design goal.

3.3 Target Estimation

For regularization methods, directly using the noisy labels as target distribution in loss function is less effective as the limited number of clean samples makes the model not rich enough to generalize effectively to the held-out data, especially at the high noise level. To yield better performance, ELR [7]

Algorithm 1 Noise Attention Learning (NAL) pseudocode

Input: DNN $\mathcal{N}_\theta$; Training set $\hat{D} = \{(\boldsymbol{x}^{[i]}, \hat{\boldsymbol{y}}^{[i]})\}_{i=1}^{N}$; Hyperparameters λ and momentum α; Total epoch E.
for epoch $e = 1$ **to** E **do**
  for each minibatch B **do**
    for i in B **do**
      Obtain $\boldsymbol{z}^{[i]}, h^{[i]} = \mathcal{N}_\theta(\boldsymbol{x}^{[i]})$.
      Obtain $\boldsymbol{p}^{[i]}, \tau^{[i]} = \texttt{softmax}(\boldsymbol{z}^{[i]}), \texttt{sigmoid}(h^{[i]})$.
      Update $\boldsymbol{t}_{[e]}^{[i]}$ by Eq. (4).
    end for
    Calculate $\mathcal{L}_{\text{NAL}} = -\frac{1}{|B|}\sum_{i=1}^{|B|}(\boldsymbol{t}_{[e]}^{[i]})^\top \log\left(\tau^{[i]}(\boldsymbol{p}^{[i]} - \boldsymbol{t}_{[e]}^{[i]}) + \boldsymbol{t}_{[e]}^{[i]}\right) - \frac{\lambda}{|B|}\sum_{i=1}^{|B|}\log(\tau^{[i]})$.
    Update θ using stochastic gradient descent.
  end for
end for
Output: θ.

use the temporal ensembling [13] to estimate targets in its regularizer and steer the model towards these new targets. The ensemble predictions are formed by an exponential moving average of historical outputs. Specifically, in the m-th epoch, it can be expressed as $\tilde{\boldsymbol{p}}_{[m]} = \sum_{j=1}^{m}(1-\alpha)\alpha^{m-j}\boldsymbol{p}_{[j]}$, where $0 \leq \alpha < 1$ is the momentum and $\boldsymbol{p}_{[j]}$ represents the output of j-th epoch. In this paper, we use the ensemble strategy in SELC [12] to estimate our targets $\boldsymbol{t}$ for the m-th epoch as follows:

$$\boldsymbol{t}_{[m]} = \underbrace{\alpha^m \hat{\boldsymbol{y}}}_{\text{initial term}} + \underbrace{\sum_{j=1}^{m}(1-\alpha)\alpha^{m-j}\boldsymbol{p}_{[j]}}_{\text{ensemble term}}. \tag{4}$$

The initial term preserves the original noisy labels with exponential decaying weights α^m. In the early learning phase (small m), the overall target relies on noisy labels to learn the model. As the learning continues (larger m), α^m approaches 0. The overall target eventually depends on the ensemble term $\tilde{\boldsymbol{p}}_{[m]}$ and penalizes model predictions that are inconsistent with this target. In our experiment, we will demonstrate that estimated targets are more accurate than original noisy labels. We simply replace noisy label $\hat{\boldsymbol{y}}$ with ensemble target $\boldsymbol{t}$ in our loss. Algorithm 1 shows pseudocode of our method.

4 Theoretical Justification

In this section, we demonstrate the noise robustness of $\mathcal{L}_{\text{NAL}}$ by analyzing how it scales the gradients accordingly to prevent memorization of mislabeled samples. The omitted proofs in this section are in Appendix A. For clarity of explanation, we denote the true label of sample $\boldsymbol{x}$ as $y \in \{1, ..., K\}$. The ground-truth distribution over labels for sample $\boldsymbol{x}$ is $q(y|\boldsymbol{x})$, and $\sum_{k=1}^{K} q(k|\boldsymbol{x}) = 1$. Consider the case of a single ground-truth label y, then $q(y|\boldsymbol{x}) = 1$ and $q(k|\boldsymbol{x}) = 0$ for all $k \neq y$. We denote the prediction probability as $p(k|\boldsymbol{x})$ and $\sum_{k=1}^{K} p(k|\boldsymbol{x}) = 1$. For notation simplicity, we denote p_k, q_k, p_y, q_y, p_j, q_j as abbreviations for $p(k|\boldsymbol{x})$, $q(k|\boldsymbol{x})$, $p(y|\boldsymbol{x})$, $q(y|\boldsymbol{x})$, $p(j|\boldsymbol{x})$ and $q(j|\boldsymbol{x})$, where j represents j-th entry. First, we show how the CE loss fails in noisy-label scenario.

Lemma 4.1. *Given the cross-entropy loss $\mathcal{L}_{ce}$ in Eq. (1), we rewrite the sample-wise loss $\ell_{ce} = -\sum_{k=1}^{K} q_k \log p_k$. Its gradient with respect to z_j is*

$$\frac{\partial \ell_{ce}}{\partial z_j} = \begin{cases} p_j - 1 \leq 0, & q_j = q_y = 1 \ (j \text{ is the true class for } \boldsymbol{x}), \\ p_j \geq 0, & q_j = 0 \ (j \text{ is not the true class for } \boldsymbol{x}), \end{cases} \tag{5}$$

where z_j is the j-th entry of logits $\boldsymbol{z}$. $q_j = q_y = 1$ means j equals the true class y.

In clean-label scenario, Lemma 4.1 ensures that, during SGD, learning direction of CE loss continues towards the true class as the corresponding gradient remains negative. However, in noisy-label scenario, the learning direction fluctuates. Suppose j is true class and equals y, but $q_j = 0$ due to the label noise, then the contribution of a mislabeled sample to the gradient is reversed (i.e. gradient

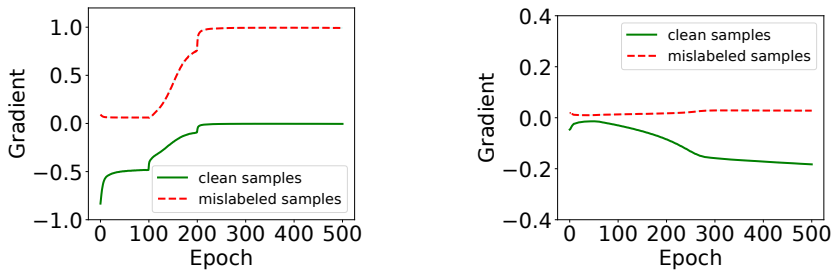

(a) Gradient of $\mathcal{L}_{\text{ce}}$ (b) Gradient of $\mathcal{L}_{\text{NAL}}$

Figure 3: The results of gradient on CIFAR-10 with 40% symmetric label noise using ResNet34. We observe that in plot (a), the gradient of clean samples dominates in early learning stage, but afterwards it vanishes (close to 0) and the gradient of mislabeled samples dominates. In plot (b), NAL effectively keeps the gradient of clean samples dominant and diminishes the gradient of mislabeled samples.

should be negative but get positive instead). The entry corresponding to the impostor class j', is also reversed because $q_{j'} = 1$, causing the gradient of mislabeled samples dominates (in Figure 3(a)). Consequently, training with CE loss results in memorization of the mislabeled samples.

Theorem 4.1. *Given the noise attention loss $\mathcal{L}_{NAL}$ in Eq. (3), we rewrite the sample-wise loss $\ell_{NAL} = -\sum_{k=1}^{K} q_k \log(\tau(p_k - q_k) + q_k) - \lambda \log \tau$. Its gradient with respect to the logits z_j can be derived as*

$$\frac{\partial \ell_{NAL}}{\partial z_j} = \begin{cases} \dfrac{p_y}{p_y - 1 + 1/\tau}(p_j - 1) \leq 0, & q_j = q_y = 1 \ (j \textit{ is the true class for } \boldsymbol{x}), \quad (6a) \\ \dfrac{p_y}{p_y - 1 + 1/\tau} p_j \geq 0, & q_j = 0 \ (j \textit{ is not the true class for } \boldsymbol{x}), \quad (6b) \end{cases}$$

where the multiplier $\frac{p_y}{p_y - 1 + 1/\tau} \in (0, 1)$.

Theorem 4.1 ensures that learning on true class persists when training with noise attention loss. In addition, compared to the gradient of ℓ_{ce}, the gradient of ℓ_{NAL} is scaled by an positive multiplier term $\frac{p_y}{p_y - 1 + 1/\tau}$. Let's denote $\varphi = \frac{p_y}{p_y - 1 + 1/\tau}$. φ is monotonically increasing on τ. We have $\lim_{\tau \to 1} \varphi = 1$, and $\lim_{\tau \to 0} \varphi = 0$. For the samples with the true class j in Eq. (6a), the cross-entropy gradient term $p_j - 1$ of clean samples tends to vanish after early learning stage, causing mislabeled samples to dominate the gradient. However, by multiplying φ (note that $\varphi \to 0$ for mislabeled samples and $\varphi \to 1$ for clean samples due to attention weight distribution), it counteracts the effect of gradient dominating by mislabeled samples. For the samples that j is not the true class in Eq. (6b), the gradient term p_j is positive. Multiplying $\varphi < 1$ effectively dampens the magnitudes of coefficients on these mislabeled samples, thereby diminishing their effect on the gradient. Figure 3(b) empirically shows the gradient when training with $\mathcal{L}_{\text{NAL}}$. It can be observed that NAL keeps the gradient of clean samples dominant and diminishes the gradient of mislabeled samples when epoch increases, effectively preventing memorization of mislabeled samples.

5 Experiments

In this section, we first compare NAL with the existing methods on five widely used datasets. Then we provide several empirical results towards a better understanding of NAL. We also provide an ablation study to evaluate the influence of each component and show the results when integrated with another noise robust method SCE [23]. Finally, we discuss the scenarios when NAL encounters hard samples. All experiments are implemented in PyTorch and run in a single NIVDIA A100 GPU.

5.1 Comparison with Existing Methods

Datasets and Setups. We evaluate our approach on two benchmarks CIFAR-10 and CIFAR-100 [2] with simulated label noise, and three real-world datasets, ANIMAL-10N [15], Clothing1M [16] and WebVision [3]. Since CIFAR-10 and CIFAR-100 are initially clean, we follow [18] to inject

Table 1: Test Accuracy (%) on CIFAR-10 and CIFAR-100 with various levels of label noise injected to the training set. We compare with previous works under the same backbone ResNet34. The results are averaged over 3 trials. Results are taken from their original papers. The best results are in **bold**.

Dataset	CIFAR-10					CIFAR-100				
Noise type	symm				asymm	symm				asymm
Noise ratio	20%	40%	60%	80%	40%	20%	40%	60%	80%	40%
Cross Entropy	86.98 ± 0.12	81.88 ± 0.29	74.14 ± 0.56	53.82 ± 1.04	80.11 ± 1.44	58.72 ± 0.26	48.20 ± 0.65	37.41 ± 0.94	18.10 ± 0.82	42.74 ± 0.61
Forward $\hat{T}$ [18]	87.99 ± 0.36	83.25 ± 0.38	74.96 ± 0.65	54.64 ± 0.44	83.55 ± 0.58	39.19 ± 2.61	31.05 ± 1.44	19.12 ± 1.95	8.99 ± 0.58	34.44 ± 1.93
Bootstrap [21]	86.23 ± 0.23	82.23 ± 0.37	75.12 ± 0.56	54.12 ± 1.32	81.21 ± 1.47	58.27 ± 0.21	47.66 ± 0.55	34.68 ± 1.10	21.64 ± 0.97	45.12 ± 0.57
GCE [24]	89.83 ± 0.20	87.13 ± 0.22	82.54 ± 0.23	64.07 ± 1.38	76.74 ± 0.61	66.81 ± 0.42	61.77 ± 0.24	53.16 ± 0.78	29.16 ± 0.74	47.22 ± 1.15
Joint Opt [25]	92.25	90.79	86.87	69.16	-	58.15	54.81	47.94	17.18	-
NLNL [26]	94.23	92.43	88.32	-	89.86	71.52	66.39	56.51	-	45.70
SCE [23]	89.83 ± 0.20	87.13 ± 0.26	82.81 ± 0.61	68.12 ± 0.81	82.51 ± 0.45	70.38 ± 0.13	62.27 ± 0.22	54.82 ± 0.57	25.91 ± 0.44	69.32 ± 0.87
DAC [27]	92.91	90.71	86.30	74.84	-	73.55	66.92	57.17	32.16	-
SAT [28]	94.14	92.64	89.23	78.58	-	75.77	71.38	62.69	**38.72**	-
SELC [12]	93.09 ± 0.02	91.18 ± 0.06	87.25 ± 0.09	74.13 ± 0.14	91.05 ± 0.11	73.63 ± 0.07	68.46 ± 0.10	59.41 ± 0.06	32.63 ± 0.06	70.82 ± 0.09
ELR [7]	92.12 ± 0.35	91.43 ± 0.21	88.87 ± 0.24	80.69 ± 0.57	90.35 ± 0.38	74.68 ± 0.31	68.43 ± 0.42	60.05 ± 0.78	30.27 ± 0.86	73.73 ± 0.34
NAL (ours)	**94.37 ± 0.04**	**93.49 ± 0.07**	**90.56 ± 0.07**	**80.98 ± 0.27**	**92.09 ± 0.12**	**77.79 ± 0.28**	**74.65 ± 0.09**	**68.48 ± 0.16**	36.77 ± 0.71	**74.73 ± 0.12**

Table 2: Test accuracy (%) on CIFAR under different types of PMD noise [20]. All methods use a PreActResNet34 architecture.

Dataset	Noise	Cross Entropy	SCE [23]	LRT [29]	PLC [20]	SELC [12]	NAL (ours)
CIFAR-10	Type-I (35%)	78.11 ± 0.74	79.76 ± 0.72	80.98 ± 0.80	82.80 ± 0.27	86.97 ± 0.15	**88.81 ± 0.13**
	Type-II (35%)	76.65 ± 0.57	77.92 ± 0.89	80.74 ± 0.25	81.54 ± 0.47	87.06 ± 0.20	**87.66 ± 0.23**
	Type-III (35%)	76.89 ± 0.79	78.81 ± 0.29	81.08 ± 0.35	81.50 ± 0.50	87.31 ± 0.18	**88.57 ± 0.16**
CIFAR-100	Type-I (35%)	57.68 ± 0.29	55.20 ± 0.33	56.74 ± 0.34	60.01 ± 0.43	65.72 ± 0.17	**66.55 ± 0.16**
	Type-II (35%)	57.83 ± 0.25	56.10 ± 0.73	57.25 ± 0.68	63.68 ± 0.29	66.79 ± 0.18	**67.15 ± 0.11**
	Type-III (35%)	56.07 ± 0.79	56.04 ± 0.74	56.57 ± 0.30	63.68 ± 0.29	66.41 ± 0.17	**66.59 ± 0.40**

Table 3: The accuracy (%) results on ANIMAL-10N. All methods use an VGG-19 architecture. Results of other methods are taken from original papers.

Cross Entropy	Nested [30]	SELFIE [15]	PLC [20]	SELC [12]	Nested + Co-teaching [30]	NAL (ours)
79.40 ± 0.14	81.30 ± 0.60	81.80 ± 0.09	83.40 ± 0.43	83.73 ± 0.06	84.10 ± 0.10	**84.18 ± 0.19**

Table 4: The accuracy (%) results on Clothing1M. All compared methods use the ResNet-50 pretrained on ImageNet. The marker ‡ denotes the model is trained from scratch.

Cross Entropy	SCE [23]	DMI [31]	ODNL [32]	ELR [7]	FINE [33]	Nested [30]	HOC [34]	NAL‡ (ours)
69.21	71.02	72.46	72.47	72.87	72.91	73.10	73.39	**73.58**

Table 5: The accuracy (%) results on (mini) Webvision. Results of other methods are taken from their original papers. All methods use an InceptionResNetV2 architecture.

		Co-teaching [8]	Iterative-CV [35]	CRUST [36]	ODD [37]	NCT [38]	ELR [7]	NAL (ours)
WebVision	top1	63.58	65.24	72.40	74.60	75.16	76.26	**77.41**
	top5	85.20	85.34	89.56	90.60	90.77	91.26	**92.25**
ILSVRC12	top1	61.48	61.60	67.36	57.80	71.73	68.71	**74.09**
	top5	84.70	84.98	87.84	86.30	91.61	87.84	**92.09**

class-conditional label noise: symmetric and asymmetric label noises. Symmetric noise is generated by uniformly flipping the label to one of the other class label. Asymmetric noise is a simulation of fine-grained classification, where the label flipping only occurs within very similar classes (e.g. dog $\leftrightarrow$ cat). Following PLC [20], we also evaluate NAL on Polynomial Margin Diminishing (PMD) noise, an instance-dependent noise that allows arbitrary noise strength in a wide buffer near the decision

boundary. ANIMAL-10N contains human-labeled online images for 10 animals with confusing appearance. Its estimated noise rate is 8%. Clothing1M consists of 1 million images collected from online shopping websites with labels generated from surrounding texts. Its estimated noise rate is 38.5%. WebVision contains 2.4 million images crawled from the web using the 1000 concepts in ImageNet ILSVRC12. Its estimated noise rate is 20%. For CIFAR with class-conditional noise, we use a ResNet-34 [39] and train it using SGD with a batch size of 64. For CIFAR with instance-dependent noise, we use a PreActResNet34 [14] and train it using SGD with a batch size of 128. For ANIMAL-10N, we use VGG-19 [40] with batch normalization and train it using SGD with a batch size of 128. For Clothing1M, we train a ResNet-50 [39] using SGD with a batch size of 64. For Webvision, we train a InceptionResNetV2 [41] using SGD with a batch size of 32. More training details can be found in Appendix B.

Table 1 shows the results on CIFAR-10 and CIFAR-100 with different levels of symmetric and asymmetric label noise. We compare NAL to the best performing approaches that only modify the training loss. All of these methods use the same backbone (ResNet34). NAL shows substantial improvements over other methods and obtains the highest accuracy in most cases.

Table 2 shows the results on three types of instance-dependent (PMD) noise from PLC [20]. We observe that the proposed method outperforms baselines across different noise settings.

Table 3 shows the results on ANIMAL-10N. NAL achieves state-of-the-art performance, even better than Nested which uses Co-teaching to boost performance.

Table 4 shows the results on the Clothing1M. All compared methods are trained using ResNet50 pretrained on ImageNet. However, as NAL needs to learn the parameters W and b in the attention branch, we directly train our model from scratch. As we can observe from Table 4, NAL still slightly outperforms other methods even without using an ImageNet pretrained model.

Table 5 shows the results on the (mini) WebVision following [35]. All the compared methods are evaluated on WebVision and ImageNet ILSVRC12 validation sets. We observe that NAL consistently outperforms state-of-the-art methods on both validation sets in terms of top1 and top5 accuracy.

Note that we do not compare with some state-of-the-art methods like RoCL [42] and DivideMix [10] as baselines, because these methods are aggregations of multiple techniques (e.g. mixup [43], multiple networks [8], and complex augmentation [44]), while this paper only focuses on one, so the comparison seems unfair.

5.2 Empirical Analysis of NAL

Memorization Procedure of NAL. Figure 1(c) and 1(d) show the memorization procedure of NAL on clean and mislabeled samples, respectively. Compared to CE loss in Figure 1(a) and 1(b), NAL effectively prevents memorization of mislabeled samples, allowing the model to continue learning on the clean samples to attain high classification accuracy.

Gradient of $\mathcal{L}_{\text{ce}}$ and $\mathcal{L}_{\text{NAL}}$. Figure 3(a) and 3(b) show the gradients of CE loss and noise attention loss on CIFAR-10 with 40% symmetric noise using ResNet34 [39] respectively. In comparison to CE loss, the proposed method keeps the gradient of clean samples dominant and dampens the gradient of mislabeled samples, resulting in the whole gradient being guided by clean samples.

Attention Weights. When trained on noisy labels, we have observed that the mislabeled samples have smaller weights than the clean samples in Figure 2. Here, we report the average weights of samples in Figure 4(a). The (i, j)-th block represents the average weights of samples with clean label i and noisy label j. We observe that the attention weights on the diagonal blocks are higher than those on non-diagonal blocks, which indicates NAL does properly down-weight the mislabeled samples.

Quality of Estimated Targets. We evaluate the quality of new targets $\boldsymbol{t}$ by correction accuracy defined via $\frac{1}{N}\sum_i^N 1\{\text{argmax}_j\, \boldsymbol{y}_j^{[i]} = \text{argmax}_j\, \boldsymbol{t}_j^{[i]}\}$, where $\boldsymbol{y}^{[i]}$ is the true label of input $\boldsymbol{x}^{[i]}$. Figure 4(d) shows the correction accuracy vs. epochs on CIFAR-10 with different levels of label noise. The target estimation in Section 3.3 steadily improves the quality of new targets. Figure 4(b) and Figure 4(c) shows the confusion matrix of noisy labels and corrected labels (i.e. the hard version of new targets) w.r.t the clean labels on CIFAR-10 with 60% symmetric noise respectively. We observe that target estimation corrects the noisy labels impressively well for all classes.

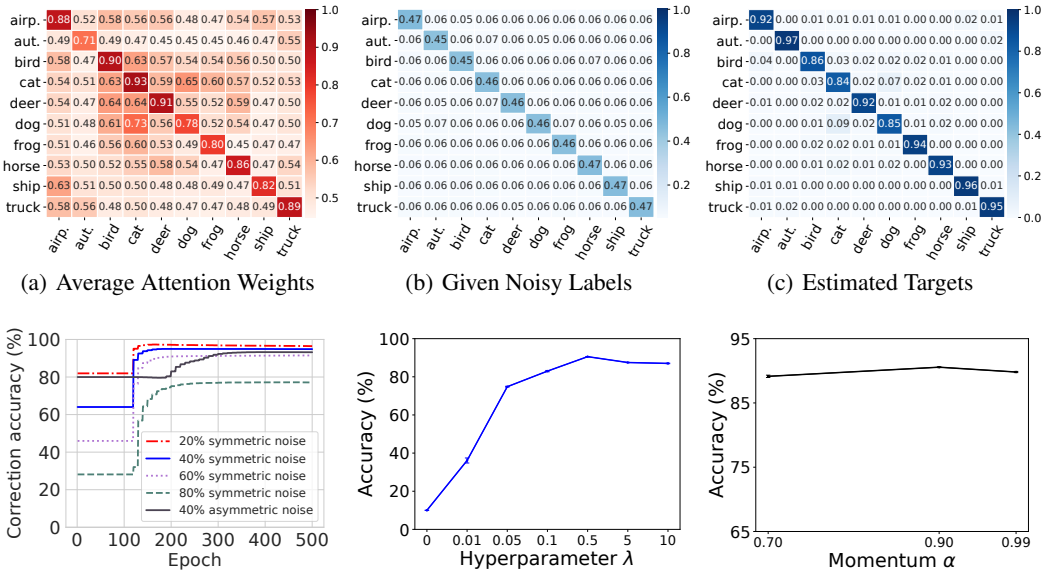

(a) Average Attention Weights (b) Given Noisy Labels (c) Estimated Targets

(d) Correction Accuracy (e) Sensitivity of λ (f) Sensitivity of α

Figure 4: (a). Average attention weights of noisy labels w.r.t clean labels on CIFAR-10 with 60% symmetric noise. (b). Confusion matrix of noisy labels w.r.t true labels on CIFAR-10 with 60% symmetric noise. (c). Confusion matrix of corrected labels w.r.t true labels on CIFAR-10 with 60% symmetric noise. (d). Label correction accuracy vs. epochs on CIFAR-10 with different levels of noise. Plots (e) and (f) show the sensitivity of λ and α on CIFAR-10 with 60% symmetric noise.

Sensitivity of Hyperparameters λ and α. NAL contains two hyperparameters: λ is the coefficient for boost term $\mathcal{L}_{\mathrm{b}}$, α is the momentum in target estimation. Figure 4(e) and 4(f) show their sensitivity to the performance. We observe that the sensitivity to α is quite mild as long as it is set close to 1. λ need to be tuned according to the complexity of dataset. It cannot be set to be very large or very small, resulting in neglecting attention term or falling into the 'lazy' learning circumstance. In our experiments, we fixed $\alpha = 0.9$ for all datasets. For CIFAR-10 and ANIMAL-10N, we set $\lambda = 0.5$. For CIFAR-100, we set $\lambda = 10$. For Webvision and Clothing1M, we set $\lambda = 50$.

5.3 Ablation Study

Table 6 reports the influence of the two components in NAL: target estimation and attention branch. Removing the target estimation leads to a significant performance drop. This suggests that using target estimation is crucial as it generates more clean samples for the model to learn. To validate the effect of the attention branch, we conduct another way to calculate the attention weights: using the confidence score (highest probability in output) as the weight, i.e., $\max_j \boldsymbol{p}_j, j \in [1, K]$. We observe that the model does not converge in hard cases. We conjecture that using the confidence from model output does interfere with the original prediction branch, while adding the attention branch to get attention weight effectively solve this problem. We also explore the possibility of integrating NAL with other methods. Here we adopt the idea from symmetric cross entropy (SCE) [23], which adds the reverse term to achieve noise robustness. As shown in Table 6, adding RNAL affects the performance under CIFAR-10, but enjoys performance boost under CIFAR-100 without extra cost.

5.4 Discussion on Hard Samples

We assume the training set consists of mislabeled samples, easy (clean) samples and hard (clean) samples. In this work, we do not design a specific technique to distinguish hard samples but the proposed NAL can handle hard samples as well. In the early learning phase, both mislabeled samples and hard samples have lower weights compared to the easy samples, which forces the model to learn only from easy samples due to gradient scaling (Theorem 4.1). After the model has learned from easy samples for a while, the model then gradually learns from hard samples rather than the mislabeled

Table 6: Ablation study results in terms of test accuracy (%) on CIFAR-10 and CIFAR-100. ⊖ means the model fails to converge. + RNAL means adding the reverse term of noise attention loss.

Dataset	CIFAR-10			CIFAR-100		
Noise type	symm		asymm	symm		asymm
Noise ratio	40%	80%	40%	40%	80%	40%
NAL	**93.49 ± 0.07**	**80.98 ± 0.27**	**92.09 ± 0.12**	74.65 ± 0.09	36.77 ± 0.71	74.73 ± 0.12
NAL w/o target estimation	89.47 ± 0.50	76.91 ± 0.22	88.23 ± 0.22	69.91 ± 0.21	31.33 ± 0.38	55.68 ± 0.17
NAL w/o attention branch	90.94 ± 0.28	⊖	91.55 ± 0.07	⊖	⊖	⊖
NAL + RNAL	92.92 ± 0.29	80.20 ± 0.42	88.17 ± 0.63	**75.38 ± 0.08**	**38.24 ± 0.55**	**74.89 ± 0.20**

samples. This is because the hard samples are more connected to the easy samples than the mislabeled samples, as the former two share some common features [45, 46]. Therefore, the proposed method can continuously learn from clean samples (both easy and hard) and prevent the memorization of mislabeled samples. In Figure 2, we can observe less overlap between clean and mislabeled samples. We also observe that some clean samples are given low weights, and some mislabeled samples are given high weights. The clean samples given low weights are actually hard clean samples. There are also mislabeled samples given high weights. These mislabeled samples are hard samples with "proper" wrong labels. For example, given a hard sample: a cat image that looks like a dog due to blurry resolution (e.g. 32×32). When generating simulated label noise, it is likely to assign a dog label for this sample. Compared to regular mislabeled samples, this kind of mislabeled samples can be learned easily by the classifier, resulting in having high weights.

6 Related Work

We briefly discuss the existing noise-robust methods that do not require a set of clean training data (as opposed to [16, 47, 48]). **Loss Correction.** Many approaches focus on correcting the loss function explicitly by estimating the noise transition matrix [49, 18, 50]. **Robust Loss Functions.** These studies develop loss functions that are robust to label noise, including $\mathcal{L}_{\text{DMI}}$ [31], MAE [51], GCE [24], SCE [23], NCE [52], TCE [53] and GJS [54]. Above two categories of methods do not utilize the early learning phenomenon. **Sample Selection** During the early learning stage, the samples with smaller loss values are more likely to be the clean samples. Based on this observation, MentorNet [55] pre-trains a mentor network for selecting small-loss samples to guide the training of the student network. Co-teaching related methods [8, 56–58] maintain two networks, and each network is trained on the small-loss samples selected by its peer network. **Label Correction** Joint Opt [25] and PENCIL [59] replace the noisy labels with soft (i.e. model probability) or hard (i.e to one-hot vector) pseudo-labels. [9] weigh the clean and mislabeled samples by fitting a two-component Beta mixture model to loss values, and corrects the labels via mixup combination. Similarly, DivideMix [10] trains two networks to separate the clean and mislabeled samples via a two-component Gaussian mixture model, and further uses MixMatch [60] to enhance the performance. **Regularization** [61] prove the gradient descent with early stopping is an effective regularization to achieve robustness to label noise. [62] *explicitly* add the regularizer based on neural tangent kernel [63] to limit the distance between the model parameters to initialization. ELR [7] estimates the target by temporal ensembling [13] and adds a regularization term to cross-entropy loss to avoid memorization. Other techniques, such as mixup augmentation [43], label smoothing [41] and weight averaging [64], can effectively improve the performance under label noise.

7 Conclusion

In this work, we propose NAL for learning with noisy labels. Our method leverages an attention branch and a noise attention loss to learn the attention weights for distinguishing the mislabeled samples from clean samples. NAL can effectively diminish the gradient of mislabeled samples, mitigating the effect of noisy labels. We also provide extensive empirical analyses and evaluate its effectiveness across multiple datasets with different types and ratios of label noises.

There are still multiple open problems for future research. Currently, label noise has been extensively studied in image classification task. Other research areas, such as graph learning and federated learning, remain to be explored. On the methodological front, we hope that our work will trigger interest in designing novel network architectures that inherently provide robustness to label noise.

References

[1] Jia Deng, Wei Dong, Richard Socher, Li-Jia Li, Kai Li, and Li Fei-Fei. Imagenet: A large-scale hierarchical image database. In *2009 IEEE conference on computer vision and pattern recognition*, pages 248–255. Ieee, 2009.

[2] Alex Krizhevsky et al. Learning multiple layers of features from tiny images. 2009.

[3] Wen Li, Limin Wang, Wei Li, Eirikur Agustsson, and Luc Van Gool. Webvision database: Visual learning and understanding from web data. *CoRR*, 2017.

[4] Xiyu Yu, Tongliang Liu, Mingming Gong, and Dacheng Tao. Learning with biased complementary labels. In *Proceedings of the European Conference on Computer Vision (ECCV)*, pages 68–83, 2018.

[5] C Zhang, S Bengio, M Hardt, B Recht, and O Vinyals. Understanding deep learning requires rethinking generalization, 2018.

[6] Devansh Arpit, Stanisław Jastrzebski, Nicolas Ballas, David Krueger, Emmanuel Bengio, Maxinder S Kanwal, Tegan Maharaj, Asja Fischer, Aaron Courville, Yoshua Bengio, et al. A closer look at memorization in deep networks. In *Proceedings of the 34th International Conference on Machine Learning-Volume 70*, pages 233–242. JMLR. org, 2017.

[7] Sheng Liu, Jonathan Niles-Weed, Narges Razavian, and Carlos Fernandez-Granda. Early-learning regularization prevents memorization of noisy labels. *Advances in Neural Information Processing Systems*, 33, 2020.

[8] Bo Han, Quanming Yao, Xingrui Yu, Gang Niu, Miao Xu, Weihua Hu, Ivor Tsang, and Masashi Sugiyama. Co-teaching: Robust training of deep neural networks with extremely noisy labels. In *Advances in neural information processing systems*, pages 8527–8537, 2018.

[9] Eric Arazo, Diego Ortego, Paul Albert, Noel O'Connor, and Kevin Mcguinness. Unsupervised label noise modeling and loss correction. In *Proceedings of the 36th International Conference on Machine Learning*, pages 312–321, 2019.

[10] Junnan Li, Richard Socher, and Steven CH Hoi. Dividemix: Learning with noisy labels as semi-supervised learning. *International Conference on Learning Representations*, 2020.

[11] Geoff Pleiss, Tianyi Zhang, Ethan Elenberg, and Kilian Q Weinberger. Identifying mislabeled data using the area under the margin ranking. *Advances in Neural Information Processing Systems*, 33:17044–17056, 2020.

[12] Yangdi Lu and Wenbo He. Selc: Self-ensemble label correction improves learning with noisy labels. *IJCAI 2022*, 2022.

[13] Samuli Laine and Timo Aila. Temporal ensembling for semi-supervised learning. *arXiv preprint arXiv:1610.02242*, 2016.

[14] Kaiming He, Xiangyu Zhang, Shaoqing Ren, and Jian Sun. Identity mappings in deep residual networks. In *European conference on computer vision*, pages 630–645. Springer, 2016.

[15] Hwanjun Song, Minseok Kim, and Jae-Gil Lee. Selfie: Refurbishing unclean samples for robust deep learning. In *International Conference on Machine Learning*, pages 5907–5915. PMLR, 2019.

[16] Tong Xiao, Tian Xia, Yi Yang, Chang Huang, and Xiaogang Wang. Learning from massive noisy labeled data for image classification. In *Proceedings of the IEEE conference on computer vision and pattern recognition*, pages 2691–2699, 2015.

[17] Nagarajan Natarajan, Inderjit S Dhillon, Pradeep K Ravikumar, and Ambuj Tewari. Learning with noisy labels. *NIPS*, 26:1196–1204, 2013.

[18] Giorgio Patrini, Alessandro Rozza, Aditya Krishna Menon, Richard Nock, and Lizhen Qu. Making deep neural networks robust to label noise: A loss correction approach. In *Proceedings of the IEEE Conference on Computer Vision and Pattern Recognition*, pages 1944–1952, 2017.

[19] Jiacheng Cheng, Tongliang Liu, Kotagiri Ramamohanarao, and Dacheng Tao. Learning with bounded instance and label-dependent label noise. In *International Conference on Machine Learning*, pages 1789–1799. PMLR, 2020.

[20] Yikai Zhang, Songzhu Zheng, Pengxiang Wu, Mayank Goswami, and Chao Chen. Learning with feature-dependent label noise: A progressive approach. In *International Conference on Learning Representations*, 2021.

[21] Scott E Reed, Honglak Lee, Dragomir Anguelov, Christian Szegedy, Dumitru Erhan, and Andrew Rabinovich. Training deep neural networks on noisy labels with bootstrapping. In *ICLR (Workshop)*, 2015.

[22] Xingjun Ma, Yisen Wang, Michael E Houle, Shuo Zhou, Sarah Erfani, Shutao Xia, Sudanthi Wijewickrema, and James Bailey. Dimensionality-driven learning with noisy labels. In *International Conference on Machine Learning*, pages 3355–3364. PMLR, 2018.

[23] Yisen Wang, Xingjun Ma, Zaiyi Chen, Yuan Luo, Jinfeng Yi, and James Bailey. Symmetric cross entropy for robust learning with noisy labels. In *Proceedings of the IEEE/CVF International Conference on Computer Vision*, pages 322–330, 2019.

[24] Zhilu Zhang and Mert Sabuncu. Generalized cross entropy loss for training deep neural networks with noisy labels. In *Advances in neural information processing systems*, pages 8778–8788, 2018.

[25] Daiki Tanaka, Daiki Ikami, Toshihiko Yamasaki, and Kiyoharu Aizawa. Joint optimization framework for learning with noisy labels. In *Proceedings of the IEEE Conference on Computer Vision and Pattern Recognition*, pages 5552–5560, 2018.

[26] Youngdong Kim, Junho Yim, Juseung Yun, and Junmo Kim. Nlnl: Negative learning for noisy labels. In *Proceedings of the IEEE International Conference on Computer Vision*, pages 101–110, 2019.

[27] Sunil Thulasidasan, Tanmoy Bhattacharya, Jeff Bilmes, Gopinath Chennupati, and Jamal Mohd-Yusof. Combating label noise in deep learning using abstention. In *International Conference on Machine Learning*, pages 6234–6243. PMLR, 2019.

[28] Lang Huang, Chao Zhang, and Hongyang Zhang. Self-adaptive training: beyond empirical risk minimization. *NeurIPS*, 2020.

[29] Songzhu Zheng, Pengxiang Wu, Aman Goswami, Mayank Goswami, Dimitris Metaxas, and Chao Chen. Error-bounded correction of noisy labels. In *ICML*, pages 11447–11457. PMLR, 2020.

[30] Yingyi Chen, Xi Shen, Shell Xu Hu, and Johan AK Suykens. Boosting co-teaching with compression regularization for label noise. In *CVPR*, pages 2688–2692, 2021.

[31] Yilun Xu, Peng Cao, Yuqing Kong, and Yizhou Wang. L_dmi: A novel information-theoretic loss function for training deep nets robust to label noise. In *NeurIPS*, pages 6222–6233, 2019.

[32] Hongxin Wei, Lue Tao, Renchunzi Xie, and Bo An. Open-set label noise can improve robustness against inherent label noise. *NIPS*, 2021.

[33] Taehyeon Kim, Jongwoo Ko, Sangwook Cho, Jinhwan Choi, and Se-Young Yun. Fine samples for learning with noisy labels. *NIPS*, 2021.

[34] Zhaowei Zhu, Yiwen Song, and Yang Liu. Clusterability as an alternative to anchor points when learning with noisy labels. In *International Conference on Machine Learning*, pages 12912–12923. PMLR, 2021.

[35] Pengfei Chen, Ben Ben Liao, Guangyong Chen, and Shengyu Zhang. Understanding and utilizing deep neural networks trained with noisy labels. In *International Conference on Machine Learning*, pages 1062–1070, 2019.

[36] Baharan Mirzasoleiman, Kaidi Cao, and Jure Leskovec. Coresets for robust training of neural networks against noisy labels. *NIPS*, 2020.

[37] Jiaming Song, Yann Dauphin, Michael Auli, and Tengyu Ma. Robust and on-the-fly dataset denoising for image classification. In *European Conference on Computer Vision*, pages 556–572. Springer, 2020.

[38] Fahad Sarfraz, Elahe Arani, and Bahram Zonooz. Noisy concurrent training for efficient learning under label noise. In *Proceedings of the IEEE/CVF Winter Conference on Applications of Computer Vision*, pages 3159–3168, 2021.

[39] Kaiming He, Xiangyu Zhang, Shaoqing Ren, and Jian Sun. Deep residual learning for image recognition. In *Proceedings of the IEEE conference on computer vision and pattern recognition*, pages 770–778, 2016.

[40] Karen Simonyan and Andrew Zisserman. Very deep convolutional networks for large-scale image recognition. *ICLR*, 2015.

[41] Christian Szegedy, Vincent Vanhoucke, Sergey Ioffe, Jon Shlens, and Zbigniew Wojna. Rethinking the inception architecture for computer vision. In *Proceedings of the IEEE conference on computer vision and pattern recognition*, pages 2818–2826, 2016.

[42] Tianyi Zhou, Shengjie Wang, and Jeff Bilmes. Robust curriculum learning: From clean label detection to noisy label self-correction. In *International Conference on Learning Representations*, 2020.

[43] Hongyi Zhang, Moustapha Cisse, Yann N Dauphin, and David Lopez-Paz. mixup: Beyond empirical risk minimization. *In International Conference on Learning Representations*, 2018b.

[44] Ekin D Cubuk, Barret Zoph, Jonathon Shlens, and Quoc V Le. Randaugment: Practical automated data augmentation with a reduced search space. In *Proceedings of the IEEE/CVF Conference on Computer Vision and Pattern Recognition Workshops*, pages 702–703, 2020.

[45] Yingbin Bai and Tongliang Liu. Me-momentum: Extracting hard confident examples from noisily labeled data. In *Proceedings of the IEEE/CVF International Conference on Computer Vision*, pages 9312–9321, 2021.

[46] Filipe R Cordeiro, Vasileios Belagiannis, Ian Reid, and Gustavo Carneiro. Propmix: Hard sample filtering and proportional mixup for learning with noisy labels. *BMVC*, 2021.

[47] Arash Vahdat. Toward robustness against label noise in training deep discriminative neural networks. In *Advances in Neural Information Processing Systems*, pages 5596–5605, 2017.

[48] Dan Hendrycks, Mantas Mazeika, Duncan Wilson, and Kevin Gimpel. Using trusted data to train deep networks on labels corrupted by severe noise. In *NeurIPS*, 2018.

[49] Jacob Goldberger and Ehud Ben-Reuven. Training deep neural-networks using a noise adaptation layer. 2016.

[50] Ryutaro Tanno, Ardavan Saeedi, Swami Sankaranarayanan, Daniel C Alexander, and Nathan Silberman. Learning from noisy labels by regularized estimation of annotator confusion. In *Proceedings of the IEEE/CVF Conference on Computer Vision and Pattern Recognition*, pages 11244–11253, 2019.

[51] Aritra Ghosh, Himanshu Kumar, and PS Sastry. Robust loss functions under label noise for deep neural networks. In *Thirty-First AAAI Conference on Artificial Intelligence*, 2017.

[52] Xingjun Ma, Hanxun Huang, Yisen Wang, Simone Romano, Sarah Erfani, and James Bailey. Normalized loss functions for deep learning with noisy labels. In *International Conference on Machine Learning*, pages 6543–6553. PMLR, 2020.

[53] Lei Feng, Senlin Shu, Zhuoyi Lin, Fengmao Lv, Li Li, and Bo An. Can cross entropy loss be robust to label noise. In *Proceedings of the 29th International Joint Conferences on Artificial Intelligence*, pages 2206–2212, 2020.

[54] Erik Englesson and Hossein Azizpour. Generalized jensen-shannon divergence loss for learning with noisy labels. *Advances in Neural Information Processing Systems*, 34, 2021.

[55] Lu Jiang, Zhengyuan Zhou, Thomas Leung, Li-Jia Li, and Li Fei-Fei. Mentornet: Learning data-driven curriculum for very deep neural networks on corrupted labels. In *International Conference on Machine Learning*, pages 2304–2313. PMLR, 2018.

[56] Xingrui Yu, Bo Han, Jiangchao Yao, Gang Niu, Ivor Tsang, and Masashi Sugiyama. How does disagreement help generalization against label corruption? In *International Conference on Machine Learning*, pages 7164–7173. PMLR, 2019.

[57] Hongxin Wei, Lei Feng, Xiangyu Chen, and Bo An. Combating noisy labels by agreement: A joint training method with co-regularization. In *Proceedings of the IEEE/CVF Conference on Computer Vision and Pattern Recognition*, pages 13726–13735, 2020.

[58] Yangdi Lu, Yang Bo, and Wenbo He. An ensemble model for combating label noise. In *Proceedings of the Fifteenth ACM International Conference on Web Search and Data Mining*, pages 608–617, 2022.

[59] Kun Yi and Jianxin Wu. Probabilistic end-to-end noise correction for learning with noisy labels. In *Proceedings of the IEEE Conference on Computer Vision and Pattern Recognition*, pages 7017–7025, 2019.

[60] David Berthelot, Nicholas Carlini, Ian Goodfellow, Nicolas Papernot, Avital Oliver, and Colin A Raffel. Mixmatch: A holistic approach to semi-supervised learning. In *Advances in Neural Information Processing Systems*, pages 5050–5060, 2019.

[61] Mingchen Li, Mahdi Soltanolkotabi, and Samet Oymak. Gradient descent with early stopping is provably robust to label noise for overparameterized neural networks. In *International Conference on Artificial Intelligence and Statistics*, pages 4313–4324. PMLR, 2020.

[62] Wei Hu, Zhiyuan Li, and Dingli Yu. Simple and effective regularization methods for training on noisily labeled data with generalization guarantee. In *International Conference on Learning Representations*, 2019.

[63] Arthur Jacot, Franck Gabriel, and Clément Hongler. Neural tangent kernel: convergence and generalization in neural networks. In *Proceedings of the 32nd International Conference on Neural Information Processing Systems*, pages 8580–8589, 2018.

[64] Antti Tarvainen and Harri Valpola. Mean teachers are better role models: Weight-averaged consistency targets improve semi-supervised deep learning results. In *Proceedings of the 31st International Conference on Neural Information Processing Systems*, pages 1195–1204, 2017.

[65] Pengfei Chen, Junjie Ye, Guangyong Chen, Jingwei Zhao, and Pheng-Ann Heng. Robustness of accuracy metric and its inspirations in learning with noisy labels. In *Proceedings of the AAAI Conference on Artificial Intelligence*, volume 35, pages 11451–11461, 2021.

Checklist

1. For all authors...
   (a) Do the main claims made in the abstract and introduction accurately reflect the paper's contributions and scope? [Yes]
   (b) Did you describe the limitations of your work? [Yes]
   (c) Did you discuss any potential negative societal impacts of your work? [No] Our work advances the development of deep learning methods and is useful because the accurate annotations are hard and expensive to gather in practice. Currently, we do not find any potential negative societal impacts.
   (d) Have you read the ethics review guidelines and ensured that your paper conforms to them? [Yes]
2. If you are including theoretical results...
   (a) Did you state the full set of assumptions of all theoretical results? [Yes] See Appendix in supplementary materials.
   (b) Did you include complete proofs of all theoretical results? [Yes] See Appendix in supplementary materials.
3. If you ran experiments...
   (a) Did you include the code, data, and instructions needed to reproduce the main experimental results (either in the supplemental material or as a URL)? [Yes] The code is included in supplementary material. Two datasets CIFAR-10 and CIFAR-100 will be automatically downloaded when you run the code. The information of ANIMAL-10N, Clothing1M and Webvision dataset can be found online.
   (b) Did you specify all the training details (e.g., data splits, hyperparameters, how they were chosen)? [Yes]
   (c) Did you report error bars (e.g., with respect to the random seed after running experiments multiple times)? [Yes] We run experiments in three times with different random seeds.
   (d) Did you include the total amount of compute and the type of resources used (e.g., type of GPUs, internal cluster, or cloud provider)? [Yes] See Appendix.
4. If you are using existing assets (e.g., code, data, models) or curating/releasing new assets...
   (a) If your work uses existing assets, did you cite the creators? [Yes] We cite the papers when using the datasets.
   (b) Did you mention the license of the assets? [No] The datasets used in this paper are public.
   (c) Did you include any new assets either in the supplemental material or as a URL? [No]
   (d) Did you discuss whether and how consent was obtained from people whose data you're using/curating? [N/A]
   (e) Did you discuss whether the data you are using/curating contains personally identifiable information or offensive content? [N/A]
5. If you used crowdsourcing or conducted research with human subjects...
   (a) Did you include the full text of instructions given to participants and screenshots, if applicable? [N/A]
   (b) Did you describe any potential participant risks, with links to Institutional Review Board (IRB) approvals, if applicable? [N/A]
   (c) Did you include the estimated hourly wage paid to participants and the total amount spent on participant compensation? [N/A]

A Missing Proofs

A.1 Gradient Derivation of ℓ_{NAL}

The sample-wise ℓ_{NAL} can be rewrite as:

$$\ell_{\text{NAL}} = \ell_{\text{na}} + \lambda \ell_{\text{b}} = -\sum_{k=1}^{K} q_k \log(\tau(p_k - q_k) + q_k) - \lambda \log \tau. \tag{1}$$

As τ is learned from attention branch. The derivation of the ℓ_{NAL} with respect to the logits is as follows:

$$\frac{\partial \ell_{\text{NAL}}}{\partial z_j} = \frac{\partial \ell_{\text{na}}}{\partial z_j} = -\sum_{k=1}^{K} \frac{\tau q_k}{\tau(p_k - q_k) + q_k} \frac{\partial p_k}{\partial z_j}. \tag{2}$$

Since $p_k = \texttt{softmax}(\boldsymbol{z})$=$\frac{e^{z_k}}{\sum_{j=1}^{K} e^{z_j}}$, we have

$$\frac{\partial p_k}{\partial z_j} = \frac{\partial \left(\frac{e^{z_k}}{\sum_{j=1}^{K} e^{z_j}}\right)}{\partial z_j} = \frac{\frac{\partial e^{z_k}}{\partial z_j}(\sum_{j=1}^{K} e^{z_j}) - e^{z_k} \frac{\partial \left(\sum_{j=1}^{K} e^{z_j}\right)}{\partial z_j}}{(\sum_{j=1}^{K} e^{z_j})^2}. \tag{3}$$

In the case of $k = j$:

$$\begin{aligned}\frac{\partial p_k}{\partial z_j} =& \frac{\frac{\partial e^{z_k}}{\partial z_k}(\sum_{k=1}^{K} e^{z_k}) - e^{z_k} \frac{\partial \left(\sum_{k=1}^{K} e^{z_k}\right)}{\partial z_k}}{(\sum_{k=1}^{K} e^{z_k})^2} = \frac{e^{z_k}(\sum_{k=1}^{K} e^{z_k}) - e^{z_k} \cdot e^{z_k}}{(\sum_{k=1}^{K} e^{z_k})^2} \\ =& \frac{e^{z_k}}{\sum_{k=1}^{K} e^{z_k}} - \left(\frac{e^{z_k}}{\sum_{k=1}^{K} e^{z_k}}\right)^2 = p_k - p_k^2.\end{aligned} \tag{4}$$

In the case of $k \neq j$:

$$\frac{\partial p_k}{\partial z_j} = \frac{0 \cdot (\sum_{j=1}^{K} e^{z_j}) - e^{z_k} \cdot e^{z_j}}{(\sum_{j=1}^{K} e^{z_j})^2} = -\frac{e^{z_k}}{\sum_{j=1}^{K} e^{z_j}} \frac{e^{z_j}}{\sum_{j=1}^{K} e^{z_j}} = -p_k p_j. \tag{5}$$

Combining Eq. (4) and (5) into Eq. (2), we obtain:

$$\begin{aligned}\frac{\partial \ell_{\text{NAL}}}{\partial z_j} =& -\sum_{k=1}^{K} \frac{\tau q_k}{\tau(p_k - q_k) + q_k} \frac{\partial p_k}{\partial z_j} \\ =& -\frac{\tau q_j}{\tau(p_j - q_j) + q_j} \frac{\partial p_j}{\partial z_j} - \sum_{k \neq j}^{K} \frac{\tau q_k}{\tau(p_k - q_k) + q_k} \frac{\partial p_k}{\partial z_j} \\ =& -\frac{\tau q_j}{\tau(p_j - q_j) + q_j}(p_j - p_j^2) - \sum_{k \neq j}^{K} \frac{\tau q_k}{\tau(p_k - q_k) + q_k}(-p_k p_j) \\ =& -\frac{\tau q_j p_j}{\tau(p_j - q_j) + q_j} + p_j \sum_{k=1}^{K} \frac{\tau q_k p_k}{\tau(p_k - q_k) + q_k}.\end{aligned} \tag{6}$$

Therefore, if $q_j = q_y = 1$, then

$$\frac{\partial \ell_{\text{NAL}}}{\partial z_j} = -\frac{\tau p_j}{\tau p_j - \tau + 1} + p_j \frac{\tau q_j p_j}{\tau(p_j - 1) + 1} = (p_j - 1)\frac{\tau p_j}{\tau p_j - \tau + 1} = (p_j - 1)\frac{p_j}{p_j - 1 + 1/\tau}. \tag{7}$$

If $q_j = 0$, then

$$\frac{\partial \ell_{\text{NAL}}}{\partial z_j} = p_j \frac{\tau q_y p_y}{\tau(p_y - q_y) + q_y} = p_j \frac{p_y}{p_y - 1 + 1/\tau}. \tag{8}$$

A.2 Formal Proofs for Theorem 4.1

Theorem A.1 (4.1). *Given the noise attention loss $\mathcal{L}_{NAL}$, we rewrite the sample-wise loss $\ell_{NAL} = -\sum_{k=1}^{K} q_k \log(\tau(p_k - q_k) + q_k) - \lambda \log \tau$. Its gradient with respect to the logits z_j can be derived as*

$$\frac{\partial \ell_{NAL}}{\partial z_j} = \begin{cases} \dfrac{p_y}{p_y - 1 + 1/\tau}(p_j - 1) \leq 0, & q_j = q_y = 1 \text{ (} j \text{ is the true class for } \boldsymbol{x}\text{)} \quad \text{(9a)} \\ \dfrac{p_y}{p_y - 1 + 1/\tau} p_j \geq 0, & q_j = 0 \text{ (} j \text{ is not the true class for } \boldsymbol{x}\text{)} \quad \text{(9b)} \end{cases}$$

where the multiplier $\frac{p_y}{p_y - 1 + 1/\tau} \in (0, 1)$.

Proof. From the Appendix A.1, we obtain the gradient of the sample-wise ℓ_{NAL} with respect to the logits z_j is

$$\frac{\partial \ell_{\text{NAL}}}{\partial z_j} = -\sum_{k=1}^{K} \frac{\tau q_k}{\tau(p_k - q_k) + q_k} \frac{\partial p_k}{\partial z_j} \tag{10}$$

where $\frac{\partial p_k}{\partial z_j}$ can be further derived base on whether $k = j$ by follows:

$$\frac{\partial p_k}{\partial z_j} = \begin{cases} p_k - p_k^2 & k = j \\ -p_j p_k & k \neq j \end{cases} \tag{11}$$

According to Eq. (10) and (11), the gradient of ℓ_{NAL} can be derived as:

$$\frac{\partial \ell_{\text{NAL}}}{\partial z_j} = \begin{cases} \frac{p_j}{p_j - 1 + 1/\tau}(p_j - 1) = \frac{p_y}{p_y - 1 + 1/\tau}(p_j - 1), & q_j = q_y = 1 \\ \frac{p_y}{p_y - 1 + 1/\tau} p_j, & q_j = 0 \end{cases} \tag{12}$$

We denote $\varphi = \frac{p_y}{p_y - 1 + 1/\tau}$. Since $p_j \leq 1$, we have $p_j - 1 \leq 0$. As $\tau \in (0, 1)$, the term $\frac{p_y}{p_y - 1 + 1/\tau} \in (0, 1)$, we have $(p_j - 1)\frac{p_y}{p_y - 1 + 1/\tau} \leq 0$ and $p_j \frac{p_y}{p_y - 1 + 1/\tau} \geq 0$. □

B Experimental Details

All experiments are implemented in PyTorch and run in a single Nvidia A100 GPU. For CIFAR-10 and CIFAR-100, we do not perform early stopping since we don't assume the presence of clean validation data. All test accuracy are recorded from the last epoch of training. For Clothing1M, it provides 50k, 14k, 10k refined clean data for training, validation and testing respectively. Note that we do not use the 50k clean data for fair comparison with existing methods. Similar to the compared methods [7, 23], we report the test accuracy when the performance on validation set is optimal. All tables of CIFAR-10/CIFAR-100 report the mean and standard deviation from 3 trails with different random seeds for different simulated noise.

B.1 Dataset Description and Preprocessing

The information of datasets are described in Table 7. CIFAR-10 and CIFAR-100 are clean datasets, we describe the label noise injection in Appendix B.2. ANIMAL-10N contains human-labeled online images for 10 animals with confusing appearance. Its estimated noise rate is 8%. Clothing1M consists of 1 million training images from 14 categories collected from online shopping websites with noisy labels generated from surrounding texts. Its noise level is estimated as 38.5%. Following [35], we use the mini WebVision dataset which contains the top 50 classes from the Google image subset of WebVision, which results in approximate 66 thousand images. The noise level of WebVision is estimated at 20% [3].

As for data preprocessing, we apply normalization and regular data augmentation (i.e. random crop and horizontal flip) on the training sets of all datasets. The cropping size is consistent with existing works [7]. Specifically, 32 for CIFAR-10 and CIFAR-100, 224 × 224 for Clothing 1M (after resizing to 256 × 256), and 227 × 227 for Webvision.

Table 7: Description of the datasets used in the experiments.

Dataset	# of train	# of val	# of test	# of classes	input size	Noise rate (%)
Datasets with clean annotation						
CIFAR-10	50K	-	10K	10	32×32	≈ 0.0
CIFAR-100	50K	-	10K	100	32×32	≈ 0.0
Datasets with real world noisy annotation						
ANIMAL-10N	50K	-	5K	10	64×64	≈ 8.0
Clothing1M	1M	14K	10K	14	224×224	≈ 38.5
(mini) Webvision	66K	-	2.5K	50	256×256	≈ 20.0

B.2 Simulated Label Noise Injection

Since the CIFAR-10 and CIFAR-100 are initially clean, we follow [25, 18] for symmetric and asymmetric label noise injection. Specifically, symmetric label noise is generated by randomly flipping a certain fraction of the labels in the training set following a uniform distribution. Asymmetric label noise is simulated by flipping their class to another certain class according to the mislabel confusions in the real world. For CIFAR-10, the asymmetric noisy labels are generated by mapping *truck* $\rightarrow$ *automobile*, *bird* $\rightarrow$ *airplane*, *deer* $\rightarrow$ *horse* and *cat* $\leftrightarrow$ *dog*. For CIFAR-100, the noise flips each class into the next, circularly within super-classes.

B.3 Training Procedure

CIFAR with class-conditional noise: We use a ResNet-34 and train it using SGD with a momentum of 0.9, a weight decay of 0.001, and a batch size of 64. The network is trained for 500 epochs for both CIFAR-10 and CIFAR-100. We use the cosine annealing learning rate where the maximum number of epoch for each period is 10, the maximum and minimum learning rate is set to 0.02 and 0.001 respectively. Note that the reason that we train the model 500 epochs in total is not because of the slow convergence (Our method actually converges around 250 epochs, shown in Section E). Instead, it is to fully evaluate whether the proposed method will overfit mislabeled samples, which avoids the interference caused by early stopping [61].

CIFAR with instance-dependent noise: We evaluate NAL on three types of label noise from the PMD noise family for consistency with PLC [20]. We use the same network architecture PreAct ResNet34 [14] as PLC. We use SGD with a momentum of 0.9 and a weight decay of 5×10^{-4}. Models are trained for 150 epochs with a batch size of 128. The learning rate is initialized as 0.1 and is divided by 5 after 60 and 120 epochs.

ANIMAL-10N: Following [15], we use VGG-19 with batch normalization and train it using SGD with a weight decay 0.001, batch size 128 and initial learning rate 0.1, which is reduced by a factor of 5 after 50 and 75 epochs (100 epochs in total).

Clothing1M: Following [16, 23], we use a ResNet-50 without pretrained parameters. We train the model with batch size 64. The optimization is done using SGD with a momentum 0.9, and weight decay 0.001. We use the same cosine annealing learning rate as CIFAR-10 except the minimum learning rate is set to 0.0001 and total epoch is 250. For each epoch, we sample 2000 mini-batches from the training data ensuring that the classes of the noisy labels are balanced.

Webvision: Following [10, 7], we use an InceptionResNetV2 as the backbone architecture. All other optimization details are the same as for CIFAR-10, except for the weight decay (0.0005) and the batch size (32).

B.4 Hyperparameters Selection and Sensitivity

We perform hyperparameter tuning via grid search: $\lambda = [0.1, 0.5, 5, 10, 50]$ and $\alpha = [0.7, 0.9, 0.99]$ using a noisy validation set sampled from the noisy training set (Note that the reason why a noisy validation set works has been empirically explored in [7] and theoretically proved in [65]). In our experiments, we set $\alpha = 0.9$ for all datasets. For CIFAR-10, we set $\lambda = 0.5$. For CIFAR-100, we set $\lambda = 10$. For ANIMAL-10N, we set $\lambda = 0.5$. For Webvision and Clothing1M, we set $\lambda = 50$.

C More Results on Training Clothing1M from Scratch

Existing methods use the ResNet-50 pretrained on ImageNet. Here we report the results when existing methods train the model from scratch in Table 4. We run the official code of SCE, SELC, DivideMix and ELR+. SCE [23] is a noise robust loss function. SELC [12] is a label correction method. These two methods only focus on modifying the loss function, thus no extra GPU space is required. In contrast, DivideMix and ELR+ (i.e. an improved version of ELR) are complex method that use multiple techniques to boost their performance. Both of them use the two networks and mixup augmentations. Other technique, such as weight average is also applied in ELR+. Therefore, more GPU space is required for DivideMix and ELR+. As we can observe in Table 8, the proposed method NAL still outperforms these methods when training the ResNet-50 from scratch.

Table 8: The accuracy (%) results on Clothing1M. The marker † denotes the methods use ResNet-50 pretrained on ImageNet. The marker ‡ denotes the model is trained from scratch.

Method	Batch Size	Required GPU Memory	Accuracy
SCE† [23]	64	7.39 GB	71.02
SCE‡ [23]	64	7.39 GB	69.40
SELC† [12]	64	7.39 GB	74.01
SELC‡ [12]	64	7.39 GB	72.02
ELR† [7]	64	-	72.87
ELR+† [7]	64	21.70 GB	74.81
ELR+‡ [7]	64	21.70 GB	72.80
DivideMix† [10]	32	19.03 GB	74.76
DivideMix‡ [10]	32	19.03 GB	70.29
NAL‡ (ours)	64	7.46 GB	73.58

D More results of Estimated Targets

We report the confusion matrix for other levels of label noise (symmetric 40%, 80% and asymmetric 40%) on CIFAR-10. Figure 5, Figure 7 and Figure 9 display the confusion matrix of noisy labels w.r.t. the clean labels on CIFAR-10 with 40% symmetric, 80% symmetric and 40% asymmetric label noise respectively. Figure 6, Figure 8 and Figure 10 display the confusion matrix of corrected labels w.r.t. the clean labels on CIFAR-10 with 40% symmetric, 80% symmetric and 40% asymmetric label noise after using the proposed method, respectively. As we can observe, the corrected labels (estimated targets) yield better quality than the original noisy labels, even under the extreme label noise (e.g. 80% symmetric noise).

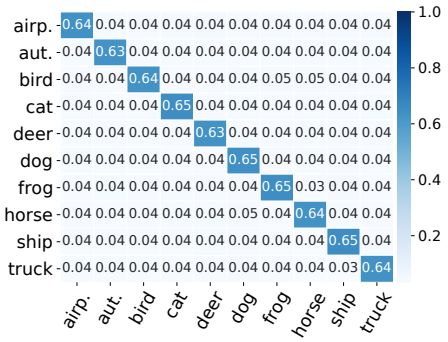

Figure 5: Confusion matrix of noisy labels w.r.t clean labels on CIFAR-10 with 40% symmetric label noise.

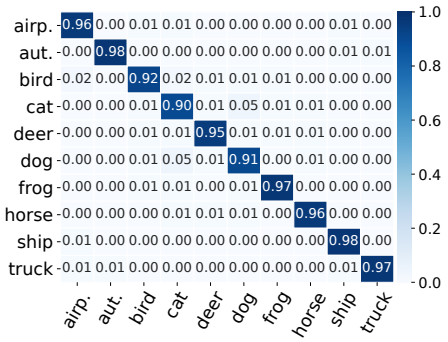

Figure 6: Confusion matrix of corrected labels w.r.t clean labels on CIFAR-10 with 40% symmetric label noise.

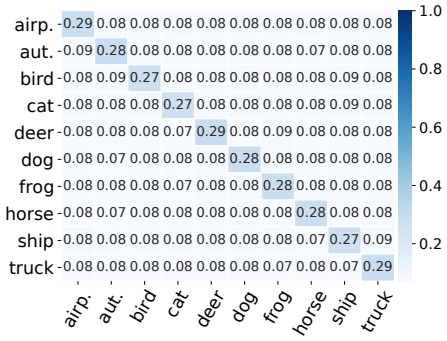

Figure 7: Confusion matrix of noisy labels w.r.t clean labels on CIFAR-10 with 80% symmetric label noise.

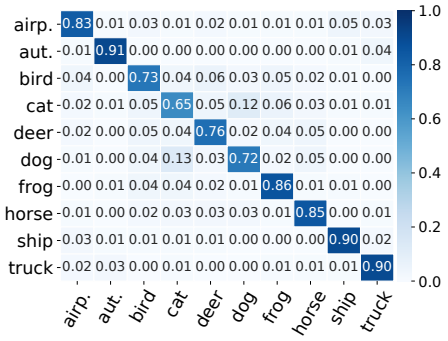

Figure 8: Confusion matrix of corrected labels w.r.t clean labels on CIFAR-10 with 80% symmetric label noise.

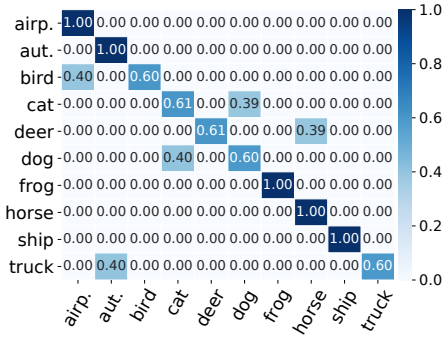

Figure 9: Confusion matrix of noisy labels w.r.t clean labels on CIFAR-10 with 40% asymmetric label noise.

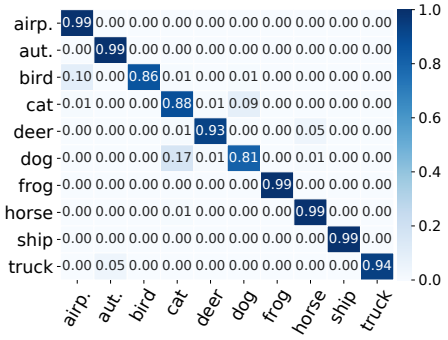

Figure 10: Confusion matrix of corrected labels w.r.t clean labels on CIFAR-10 with 40% asymmetric label noise.

E Accuracy Curves versus Epochs

In this section, we show the accuracy curves during training to show the noise robustness of NAL. As we can observe in Figure 11, CE fits the whole noisy labels eventually, while NAL only fits around 60% training samples. In Figure 12, the test accuracy of CE decreases due to memorization of noisy labels, while NAL won't. We also observe the similar results on CIFAR-10.

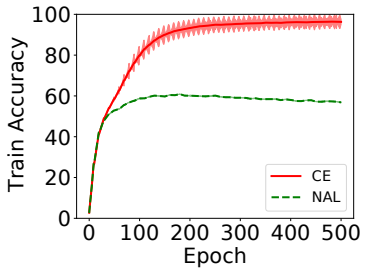

Figure 11: Train accuracy vs. epochs on CIFAR-100 with 40% symmetric label noise.

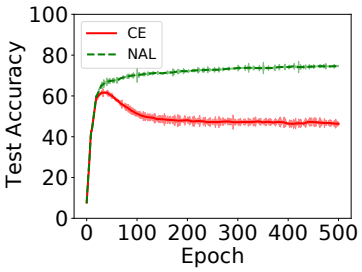

Figure 12: Test accuracy vs. epochs on CIFAR-100 with 40% symmetric label noise.

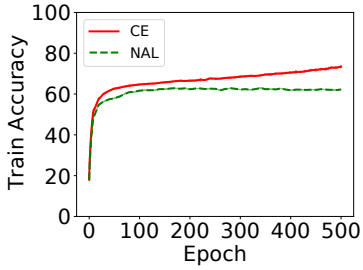

Figure 13: Train accuracy vs. epochs on CIFAR-10 with 40% symmetric label noise.

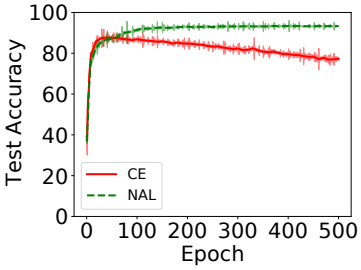

Figure 14: Test accuracy vs. epochs on CIFAR-10 with 40% symmetric label noise.

F Movement of weight τ Distribution

We monitor the weight τ distribution during training on CIFAR-10 with 40% symmetric noise using NAL. Figure 15 to Figure 17 show the results. We summarize the weight τ distribution into three stages. As can be observed, in the stage 1, clean samples and mislabeled samples have the similar τ. By continuing to train the model with NAL, the weights for clean samples and mislabeled samples start to separate. Until stage 3, the weight of clean samples is increased towards 1.0, even for most hard samples (since the weight distribution has only a little overlap between clean and mislabeled samples).

Figure 15: Stage 1

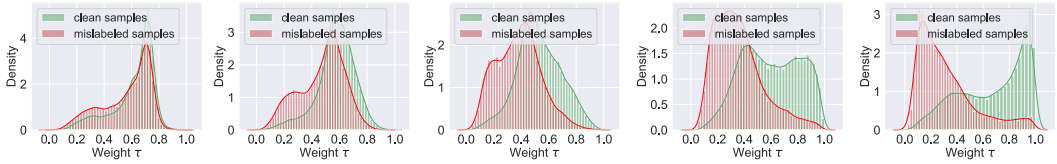

Figure 16: Stage 2

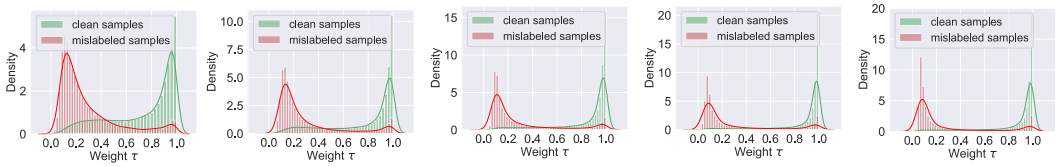

Figure 17: Stage 3